Coordination of Lower Limb During Gait in Individuals With Unilateral Transfemoral Amputation

Mingyu Hu, Yufan He, Genki Hisano, Hiroaki Hobara, and Toshiki Kobayashi

***Abstract*— Understanding the lower-limb coordination of individuals with unilateral transfemoral amputation (uTFA) while walking is essential to understand their gait mechanisms. Continuous relative phase (CRP) analysis provides insights into gait coordination patterns of the neuromusculoskeletal system based on movement kinematics. Fourteen individuals with uTFA and their age-matched non-disabled individuals participated in this study. Kinematic data of the lower limbs of the participants were collected during walking. The joint angles, segment angles, and CRP values of the thigh-shank and shank-foot couplings were investigated. The curves among the lower limbs of the participants were compared using a statistical parametric mapping test. Compensatory strategies were found in the lower limbs from coordination patterns. In thigh-shank coupling, although distinct coordination traits in stance and swing phases among the lower limbs were found, the lower limbs in both groups were discovered to remain in a similar coordination pattern during gait. For individuals with uTFA, in shank-foot coupling, intact limbs demonstrated a short period of foot-leading pattern which was significantly different from that of the other limbs during mid-stance to compensate for the weaker force generation by prosthetic limbs. The findings offer normative coordination patterns on the walking of individuals with uTFA, which could benefit prosthetic gait rehabilitation and development.**

***Index Terms*— Amputee, continuous relative phase (CRP), gait rehabilitation, prosthetic, walk.**

Manuscript received 27 June 2023; revised 28 August 2023; accepted 14 September 2023. Date of publication 18 September 2023; date of current version 3 October 2023. This work was supported in part by the Japan Society for the Promotion of Science (JSPS) KAKENHI under Grant 26702027. *(Corresponding author: Toshiki Kobayashi.)*

This work involved human subjects or animals in its research. Approval of all ethical and experimental procedures and protocols was granted by the National Institute of Advanced Industrial Science and Technology (AIST) Institutional Review Board, and performed in line with the Declaration of Helsinki (1983).

Mingyu Hu, Yufan He, and Toshiki Kobayashi are with the Department of Biomedical Engineering, Faculty of Engineering, The Hong Kong Polytechnic University, Hong Kong, China (e-mail: toshiki.kobayashi@polyu.edu.hk).

Genki Hisano is with the Faculty of Advanced Engineering, Tokyo University of Science, Tokyo 125-8585, Japan, and also with the Japan Society for the Promotion of Science (JSPS), Tokyo 102-0083, Japan.

Hiroaki Hobara is with the Faculty of Advanced Engineering, Tokyo University of Science, Tokyo 125-8585, Japan (e-mail: hobara-hiroaki@rs.tus.ac.jp).

This article has supplementary downloadable material available at https://doi.org/10.1109/TNSRE.2023.3316749, provided by the authors.

Digital Object Identifier 10.1109/TNSRE.2023.3316749

I. Background

WALKING ability is generally restored using prostheses in individuals with unilateral transfemoral amputation (uTFA). However, their gait is typically characterized as functional asymmetries in the lower limbs that are significantly different from those of non-disabled individuals [1], [2]. These gait asymmetries include different force generation, stance phase duration, and varied joint angles between the lower limbs [2], [3], [4], [5]. Some of these asymmetries are attributed to compensation mechanisms. Due to the loss of some major muscles and bones, the amputated side has limited force generation that adversely impacts kinetic parameters [6]. Additionally, the residual limb inside the prosthetic socket might not be able to bear high pressure during gait [7]. The intact limb hence compensates for the weaker force generation of the prosthetic limb by producing larger progression force and impulses during walking [2]. Kinematically, the limited prosthetic knee flexion during the swing phase is compensated by a greater hip motion of the intact limb, which causes an extended duration of the stance phase of the intact limb [5]. The quality of life in individuals with uTFA depends highly on the quality of prosthetic gait rehabilitation and the comfort of prostheses [4]. A deeper understanding of the prosthetic gait profile could benefit both prosthetic gait rehabilitation and prosthesis design, ultimately improving the quality of life for individuals with uTFA using prostheses.

Individuals with uTFA develop adapted gait patterns due to limb loss. The direct description of a movement is not viable and one solution is to build a complex human neuromusculoskeletal system using dynamic system theory [8]. During gait, the human neuromusculoskeletal system can be treated as a complete system with energy exchange. The movement and energy exchange in the lower limbs resembles a dynamic system because it contains pendulum structures that move in a sinusoidal waveform with constant energy flux. Describing this lower-limb dynamic system only needs its current status and the changing rate [8]. The dynamic system theory provides a quantitative means to describe movement coordination, which is known as the continuous relative phase (CRP) angle [9]. The current status and the changing rate of the lower limbs can be represented by the angular displacement and the angular

velocity at this moment, respectively [8]. Dividing the lower limbs into the thigh, shank, and foot segments and calculating their angles with reference to the global coordinate system offers a more sensitive detection method as opposed to using joint angles [9]. The coordination patterns between the two segments which reflect the control strategy can be quantified by the CRP values. The mean absolute relative phase (MARP) and the deviation phase (DP) quantify the CRP patterns and the variability of the coordination patterns during a specific time or phase of the gait, respectively [9]. The coordination patterns can be distinguished by the MARP values, with high values indicating out-of-phase patterns and low values indicating in-phase patterns. For the DP value, an excessively high (low) DP indicates unstable (restricted) movement patterns [8].

The gait profile of individuals with uTFA is characterized as functional asymmetries via compensatory mechanisms. These mechanisms exist across different body parts [10]. While recent investigations focused on a single joint [6], the coupling effects or the coordination patterns of the lower limbs of individuals with uTFA are equally important. This is because the coupling effects could reveal the coordination patterns generated by the central nervous system, which might advance the understanding of the gait features of individuals with uTFA. However, very few studies have investigated the lower-limb coordination patterns in individuals with uTFA [11], [12], [13]. One study reported that a prosthetic limb exhibited a larger DP in knee-ankle coupling during the stance phase and vice versa during the swing phase of walking [13]. Another two studies applied CRP as an evaluation tool for prosthetic gait rehabilitation and prosthesis design and found changes in coordination patterns [11], [12]. However, these studies built models based on joint angles, which might not be appropriate according to the dynamic system theory [8]. The original model was built based on the segment angle, and it is preferred because the dynamic system is based on the pendulum model [14], [15]. It should be noted that the joint angles are the relative angles between two neighboring segments. However, the pendulum model needs an external reference (e.g., horizontal plane) rather than relative references [15], [16]. One study evaluated the difference between the segment and joint angles using the CRP model and demonstrated that segment angles provide more sensitive results [17].

Regarding gait patterns, the typical gait parameters are discrete and obtained from the joint angle curves. For example, the peak knee extension and flexion angles, and the range of motion values were chosen from knee angle curve during gait cycle to represent the movement of the knee joint. This method reduces the dimension of the data and extracts key information from the curve. However, it neglects the dynamic changes of the gait pattern across the gait cycle. Statistical parametric mapping (SPM) is an n-dimensional methodology for the topological analysis of smooth continuum changes associated with experimental intervention [18]. It provides a framework for the continuous statistical analysis of smooth bounded n-dimensional fields [19]. For example, the SPM reveals that individuals wearing used shoes cause significantly less knee flexion angle from 90% to 100% of the stance phase than the new shoes [20]. The CRP characterizes the coordination pattern that changes as a function of time. Hence, applying the SPM analysis of CRP is suitable.

The coordination patterns of the lower limbs of individuals with uTFA are important in prosthetic gait rehabilitation and design. However, the coordination patterns during walking based on segment angles are still unclear. The coordination curve of the gait cycle reveals the change in coordination patterns at each percentage of the gait cycle. Thus, this study aimed to understand the walking coordination patterns of lower limbs (prosthetic and intact limbs) in individuals with uTFA in reference to the lower limbs (right) of non-disabled individuals. The first hypothesis is that a prosthetic limb demonstrates a larger MARP with a smaller DP than the other two limbs (intact, and right limbs) in thigh-shank coupling because a prosthetic limb has limited synchronization with the residual limb and restricted degree of freedoms. The second hypothesis is that a prosthetic limb demonstrates a smaller MARP and DP than the other two limbs in shank-foot coupling because of the passive structure and restricted variability of a prosthetic shank and foot.

II. Methods

A. Participants

This study involved 14 individuals with uTFA or knee disarticulation and 14 non-disabled individuals with a mean (SD) age of 32.6 (10.2) years, height of 1.65 (0.10) m, weight of 60.0 (10.6) kg, amputation time of 14.1 (9.1) years, and a walking speed of 1.36 (0.16) m/s (Table I). All individuals with uTFA used ischial containment sockets while all individuals with knee disarticulation used distal bearing sockets. All participants used silicone sleeves. Of the individuals with uTFA, four had long residual limbs, five had medium residual limbs and three had short residual limbs. The residual limb length was categorized as: long when it constituted 2/3 or more of the original femur bone length; medium when it ranged from 1/3 to 2/3 of the original length; and short when it was equal to or less than 1/3 of the original length [21]. The inclusion criteria were as follows: 1) older than 18 years of age, 2) unilateral transfemoral amputation or knee disarticulation, and 3) no neurological or skeletal complications other than amputation. The 14 non-disabled individuals were selected from the Advanced Industrial Science and Technology gait database with similar age, gender, and walking speed as the individuals with uTFA group [22]. The non-disabled group has a mean (SD) age of 32.5 (9.5) years, a height of 1.69 (0.09) m, a weight of 66.9 (12.5) kg, and a walking speed of 1.36 (0.16) m/s. The study was approved by the National Institute of Advanced Industrial Science and Technology (AIST) Institutional Review Board, and it was conducted following the guidelines given in the Declaration of Helsinki (1983). All subjects were informed about the study before participation and informed consent was obtained.

B. Experimental Setting and Procedure

A 3D motion capture system (MX-T 160, Vicon, Oxford Metrics, UK) was used to record kinematic data, including 15 near-infrared cameras with a sampling rate of 200 Hz.

TABLE I
DEMOGRAPHIC DATA

Participant	Gender (M/F)	Age (y)	Height (cm)	Mass (kg)	Amputated side	Etiology	Time since amputation (y)	Walking speed (m/s)	Residual limb length	Prosthetic knee	Prosthetic feet
1	F	18	156	58.3	Right	Trauma	3.5	1.18	Middle	Total knee (Össur)	Variflex xc (Össur)
2	F	38	148.5	43.9	Right	Infection	15	1.2	Long	Intelligent (Nabtesco)	Total Concept (Össur)
3	F	19	149	43.3	Right	Sarcoma	7.5	1.2	Short	3R106 (Ottobock)	1H38 (Ottobock)
4	M	33	167	62	Left	Trauma	16	1.22	Long	3R95 (Ottobock)	J-foot (IMASEN)
5	F	32	156	47.4	Right	Trauma	6.5	1.25	Middle	Total knee (Össur)	Total Concept (Össur)
6	M	43	168	67.7	Left	Trauma	16	1.32	Middle	3R80 (Ottobock)	Variflex (Össur)
7	M	24	176	63	Left	Trauma	2.7	1.36	Long	3R95 (Ottobock)	Variflex (Össur)
8	M	21	167	56.4	Left	Cancer	18	1.36	Short	3R80 (Ottobock)	Variflex (Össur)
9	M	52	170	66.6	Left	Trauma	29	1.38	KD	Intelligent (Nabtesco)	J-foot (IMASEN)
10	M	32	180	83.7	Left	Cancer	24	1.41	KD	Genium X3 (Ottobock)	1D35 (Ottobock)
11	M	44	178.5	63.6	Right	Trauma	28	1.43	Short	3R80 (Ottobock)	Triton (Ottobock)
12	M	34	161	58.7	Left	Sarcoma	21	1.46	Middle	3R95 (Ottobock)	Variflex (Össur)
13	M	40	167	57.1	Left	Cancer	4	1.52	Long	3R106 (Ottobock)	Triton (Ottobock)
14	M	26	175	66	Right	Trauma	5.2	1.8	Middle	3R80 (Ottobock)	Reflex Rotate (Össur)
Mean	—	32.6	165.6	59.8	—	—	14	1.36	—	—	—
SD	—	10.2	10.3	10.6	—	—	9.2	0.16	—	—	—

Abbreviations: F: female; M: male; KD: knee disarticulation; SD: standard deviation; y: year. The residual limb length was categorized as: long when it constituted 2/3 or more of the original femur bone length; medium when it ranged from 1/3 to 2/3 of the original length; and short when it was equal to or less than 1/3 of the original length; Ottobock located in Duderstadt Germany; Össur located in Reykjavík Iceland; IMASEN located in Aichi Japan.

The ground reaction force (GRF) was measured by nine walkway-embedded force plates (BP400600-1000PT and BP400600-2000PT, AMTI, Watertown, MA, USA) with a sampling rate of 2000 Hz. In total, 54 reflective markers were placed on the subjects based on the model modified from the Helen-Hayes marker set [23]. Subjects walked in a straight line along a 10 m walkway using a self-selected speed for a total of five times (Fig 1).

C. Data Collection and Analyses

All data were processed using Vicon Nexus software (Vicon Motion System, Oxford, UK). The collected ground reaction force (GRF) data were processed using a fourth-order Butterworth filter with zero lag and a cut-off frequency of 50 Hz. The timings of initial contact and toe-off were determined based on vertical GRFs above and below 16 N, respectively. All trajectory data were processed using a fourth-order Butterworth low-pass filter with a cut-off frequency of 10 Hz. The gait cycle was normalized to 101 points. The prosthetic and intact limbs of the individuals with uTFA, as well as the right (control) limbs of the non-disabled individuals, were included for statistical analyses. The lower-limb joint angles, segment angles, and CRP-related parameters were calculated for three limbs. Joint angles in the sagittal plane were used as basic joint kinematics and segmental angles were obtained to analyze coordination. Hip flexion, knee flexion, and ankle dorsiflexion were defined as positive directions for joint angles. For segment angles, a perpendicular line to the ground was defined as 0 degrees, and the anti-clockwise direction is defined as the positive direction (Fig. 1 (b)). Subsequently, the CRP patterns were examined in the following two couplings: thigh-shank and shank-foot. The range of motion of the joints and segments, peak flexion (or dorsiflexion) and extension (or plantar flexion) angles of the joints, and minimum angles of the segments were calculated for analyses as the peak values and range of motion indicate the movement limitation and flexibility during gait.

Typically, CRP can be calculated based on the angular displacement and angular velocity. Another method is the Hilbert transform which replaces the calculation of angular velocities by using the imaginary part of the angular displacement [24]. In this study, CRP was calculated by the Hilbert transform. The segment angles (θ) of each participant were normalized ($\bar{\theta}$) (eq1) and treated as a time series signal ($\theta\,(t)$) (eq2), where i and t represent the i th and the t th respective points in the analytical data. To perform the Hilbert transform ($H\,(\theta\,(t))$) of the signal, a custom-made MATLAB (2020, MathWorks, Massachusetts, Natick) script was employed in the previous step (eq3) and (eq4), where j denotes the imaginary part. The MATLAB 'unwarp' function was utilized to calculate the phase angle (ϕ_{rp}) (eq5). The arctan function yielded phase angles in the range of $\pm 90°$, but for a polarized coordinate, a complete range of 360° was required. To preserve the previous value and prevent it from being confined to the $\pm 90°$ range, the unwarp function was applied. The CRP angles for the thigh-shank and shank-foot couplings were determined by subtracting the proximal phase angle ($\phi_{rp-proximal}$) from the distal phase angle ($\phi_{rp-distal}$) (eq6). If the CRP angles extended beyond $\pm 180°$, they were adjusted to $\pm 180°$ by adding or subtracting 360°. Subsequently, the MARP and DP values for each gait cycle were calculated based on the CRP values obtained in the last step (eq7) and (eq8). Where n is the number of the points in the target time series, $\phi_{ith-crp}$ and SD_i is the relative phase angle and standard deviation value

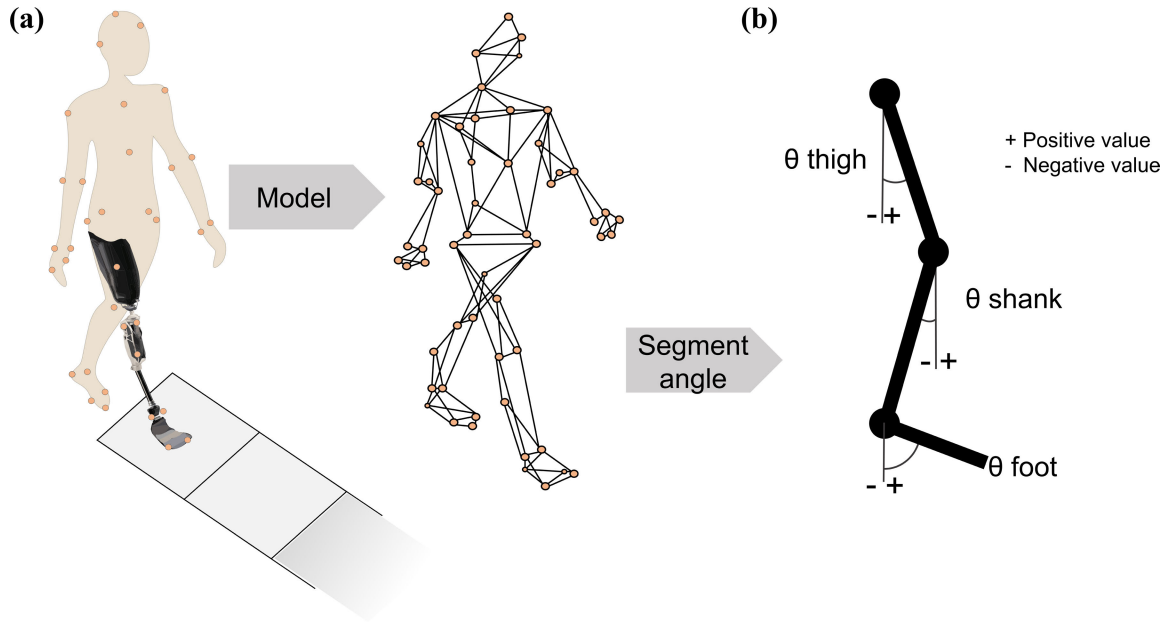

Fig. 1. Retroreflective marker locations and lower limb model (a) and the definition of the segment angles (b).

at i th points of the mean relative phase curve. A MARP evaluates the coordination pattern, while a DP represents the variability of the overall coordination at a specific time or phase within the gait cycle. A MARP (or CRP) value of 0° indicates an in-phase coordination pattern, while an increasing deviation from 0° signifies an out-of-phase relationship in the coupling [25].

$$\bar{\theta} = \theta - \min(\theta) - \left(\frac{\max(\theta) - \min(\theta)}{2}\right), \quad (1)$$

$$\theta(t) = \bar{\theta}_{(i)}, \quad i = 1, 2, \ldots, n, \quad (2)$$

$$H(t) = H(\theta(t)) = \theta(t) * \frac{1}{\pi t}, \quad (3)$$

$$\zeta(t) = \theta(t) + jH(t), \quad (4)$$

$$\phi_{rp} = \arctan\left[\frac{H(t_i)}{\theta(t_i)}\right], \quad i = 1, 2, \ldots, n, \quad (5)$$

$$\phi_{CRP} = \phi_{rp-distal} - \phi_{rp-proximal}, \quad (6)$$

$$MARP = \sum_{i=1}^{n} \frac{|\phi_{ith-crp}|}{n}, i = 1, 2, \ldots, n, \quad (7)$$

$$DP = \frac{\sum_{i=1}^{n} |SD_i|}{n}, \quad i = 1, 2, \ldots, n \quad (8)$$

The calculation of the CRP thigh-shank curve of one gait cycle was illustrated here (supplementary Fig. S1).

The positive slope of CRP curves represents the distal segment leading the movement in the phase plane, while the negative slope represents the proximal segment leading the movement in the phase plane. The thigh, shank, and foot segment angles were applied to calculate the CRP thigh-shank and CRP shank-foot. Also, MARP and DP were calculated for each CRP curve. The profiles of the joint segments and the CRP angles across the gait cycle were plotted.

In sum, eight curves including the hip, knee, ankle joint angle curves, thigh, shank, foot segment angle curves, the CRP curves of the thigh-shank, shank-foot couplings were selected from each trail and average among five gait cycles to represent the curves of each individual.

For comparing the results with other biomechanical studies, the peak values, the range of motion in the joint angle curves were selected. The minimum values and range of motion were extracted from the segment angle curves. The MARP and DP were calculated from CRP curves of thigh-shank and shank-foot couplings.

D. Statistical Analysis

For the discrete parameters, the Shapiro-Wilk test was used to determine the normality of the data. For normal distribution data, one-way ANOVA was performed to find the differences among the three lower limbs, and Bonferroni post-hoc comparison (3 comparisons) was used to correct p values and determine the differences among them. For data not presenting normal distribution, the independent-samples Kruskal-Wallis test was applied to investigate the differences. All the statistical analyses for discrete parameters were conducted by SPSS (IBM SPSS Statistics 22, SPSS Inc., Chicago, IL) and $p < 0.05$ was considered significantly different.

For the curves in this study, all curves (three joint angle curves, three segment angle curves, and two CRP angle curves) were compared using statistical parametric mapping (SPM). The One-way ANOVA test was first applied on curves from the prosthetic limbs. intact limbs, and the control limbs. Then the Bonferroni post-hoc comparison was performed to correct the p value for multiple comparisons (3 comparisons) and evaluate if there was any significant difference among the three limbs [26]. This step was conducted by modifying the open-source spm1d code (Version **0.4.18**, https://spm1d.org/) in Python (Version **3.9**) [27].

III. Results

The results of the discrete parameters in this study are shown in Table II. Three limbs (the prosthetic limbs, intact

TABLE II
MEAN VALUE, SD VALUE, NORMALITY, P-VALUE, AND POST-HOC OF THE PARAMETERS

Parameters	Limbs			Normality	p-value	Post-hoc		
	Control	Intact	Prosthetic		(Main effect)	I-C	P-C	I-P
Peak Ankle D-flex (°)	7.60 ± 2.21	7.49 ± 4.11	8.20 ± 2.36	Y	0.81	—	—	—
Peak Knee Flex (°)	63.02 ± 4.34	61.02 ± 6.18	62.73 ± 8.25	Y	0.70	—	—	—
Peak Hip Flex (°)	32.09 ± 4.33	35.94 ± 5.00	34.24 ± 5.42	Y	0.15	—	—	—
Peak Ankle P-flex (°)	25.68 ± 7.65	34.76 ± 7.50	9.54 ± 2.34	N	**<0.01***	0.27	**<0.01***	**<0.01***
Peak Knee Ext (°)	-0.61 ± 2.51	1.68 ± 2.41	1.84 ± 1.59	N	**0.04**	0.09	0.09	1.00
Peak Hip Ext (°)	17.39 ± 6.17	16.71 ± 4.05	18.35 ± 4.84	Y	0.72	—	—	—
Ankle RoM (°)	33.28 ± 6.26	42.24 ± 4.70	17.74 ± 3.25	N	**<0.01***	1.36	**<0.01***	**<0.01***
Knee RoM (°)	62.41 ± 3.13	62.70 ± 6.04	64.57 ± 8.02	Y	0.62	—	—	—
Hip RoM (°)	49.48 ± 3.77	52.66 ± 5.88	52.59 ± 5.51	Y	0.21	—	—	—
Min Thigh (°)	-20.54 ± 2.64	-21.79 ± 2.24	-22.85 ± 3.67	Y	0.14	—	—	—
Min Shank (°)	-55.58 ± 2.65	-54.16 ± 4.38	-60.22 ± 4.21	Y	**<0.01***	1.00	**0.01***	**0.01***
Min Foot (°)	-7.21 ± 7.64	-18.68 ± 6.37	3.59 ± 6.80	Y	**<0.01***	**<0.01***	**<0.01***	**<0.01***
Thigh RoM (°)	49.67 ± 3.76	52.07 ± 3.76	54.67 ± 4.45	N	**0.01***	0.60	**0.01***	0.25
Shank RoM (°)	76.94 ± 3.53	77.00 ± 4.67	84.19 ± 4.66	Y	**<0.01***	1.00	**<0.01***	**<0.01***
Foot RoM (°)	98.35 ± 7.61	112.85 ± 6.71	87.27 ± 5.14	Y	**<0.01***	**<0.01***	**<0.01***	**<0.01***
MARP thigh-shank (°)	46.72 ± 5.64	45.53 ± 5.72	53.52 ± 10.79	N	0.05	—	—	—
MARP shank-foot (°)	21.17 ± 2.53	18.93 ± 3.84	10.19 ± 3.40	Y	**<0.01***	0.28	**<0.01***	**<0.01***
DP thigh-shank (°)	2.71 ± 0.81	3.18 ± 1.34	1.73 ± 0.70	N	**<0.01***	1.00	**0.01***	**<0.01***
DP shank-foot (°)	1.75 ± 0.43	2.35 ± 0.94	0.71 ± 0.42	N	**<0.01***	0.84	**<0.01***	**<0.01***

Abbreviations: Y: Yes; N: No; Ext: extension; Flex: flexion; D-Flex: dorsiflexion; P-Flex: plantarflexion; RoM: range of motion; MARP thigh-shank: mean absolute relative phase of thigh-shank coupling; MARP shank-foot: mean absolute relative phase of shank-foot coupling; DP thigh-shank: deviation phase of thigh-shank coupling; DP shank-foot: deviation phase of shank-foot coupling. An asterisk (*) indicates a statistical significance level at $p<0.05$. C: control (right) limb of non-disabled individuals. I: the intact limb of individuals with uTFA. P: the prosthetic limb of individuals with uTFA.

limbs, and control limbs) are included in the profiles of the CRP and joint angle curves (Fig. 2, Fig. 3).

A. Coordination

There was no significant difference in the MARP of thigh-shank across all three limbs ($p = 0.05$). For shank-foot, the prosthetic limbs had significantly smaller MARP than the other limbs ($p < 0.01$, intact: 18.93 ± 3.84°, prosthetic: 10.19 ± 3.40°, control: 21.17 ± 2.5°). Regarding the DP of the thigh-shank, there were no significant differences between the intact and the control limbs. The prosthetic limbs exhibited a significantly smaller DP value when compared to the intact and control limbs ($p < 0.01$, intact: 3.18 ± 1.34°, prosthetic: 1.73 ± 0.70°, control: 2.71 ± 0.81°). In the DP of shank-foot, no significant difference was found between the control limbs and the intact limbs. However, the prosthetic limbs exhibited a significantly lower value than the intact and the control limbs ($p < 0.01$, intact: 2.35 ± 0.94°, prosthetic: 0.71 ± 0.42°, control: 1.75 ± 0.43°).

In the CRP thigh-shank curves (Fig. 2 (a)), the main differences were found between 0% to 60% of the gait cycle (Fig. 2 (a1)). During the 0% to 25% of the gait cycle, both the control and intact limbs exhibited significant differences with respect to the prosthetic limbs (Fig. 2 (a2, a4)). Significant differences were identified between the intact limbs and prosthetic limbs during 40% to 60% of the gait cycle. The intact limbs and the control limbs displayed the shank-leading pattern at the beginning of the gait cycle and changed to the thigh-leading pattern at around 10% of the gait cycle, with both limbs remaining in this pattern until 60% of the gait cycle after which they switched back to the shank-leading pattern again until the end of the gait cycle. The prosthetic limbs displayed the thigh-leading pattern until 55% of the gait cycle and switched to the shank-leading pattern until 90% of the gait cycle and changed back to the thigh-leading pattern at the end of the gait cycle. However, the last thigh-leading pattern of the prosthetic limbs only exhibits a limited significant difference from the intact and control limbs at the end of the gait cycle (Fig. 2 (a2)).

In the CRP shank-foot curves (Fig. 2 (b)), the main differences were found across the whole gait cycle with the exception of around 60% and 100% of the gait cycle (Fig. 2 (b1)). The intact and prosthetic limbs exhibited significant differences during around 5% to 20% of the gait cycle and 70% to 90% of the gait cycle (Fig. 2 (b2)). The control limbs and prosthetic limbs exhibited significant differences during 5% to 60% of the gait cycle and 65% to 90% of the gait cycle (Fig. 2 (b4)). No significant differences were observed between the intact and control limbs during the whole gait cycle except at around 20% (Fig. 2 (b3)). At the initial stance, all limbs chose the foot-leading pattern and switched to the shank-leading pattern quickly. In the mid-stance, the intact limbs exhibited a shorter period of the foot-leading pattern at 20% of the gait cycle than the other two limbs. In the swing phase, the prosthetic limbs remained in a foot-leading pattern, while the other limbs changed from foot-leading to shank-leading at around 75% of the gait cycle.

B. Kinematics

The discrete parameters are shown in Table II. In the joint and segment angles, the prosthetic limbs had a significantly smaller ankle plantar flexion angle than the other limbs

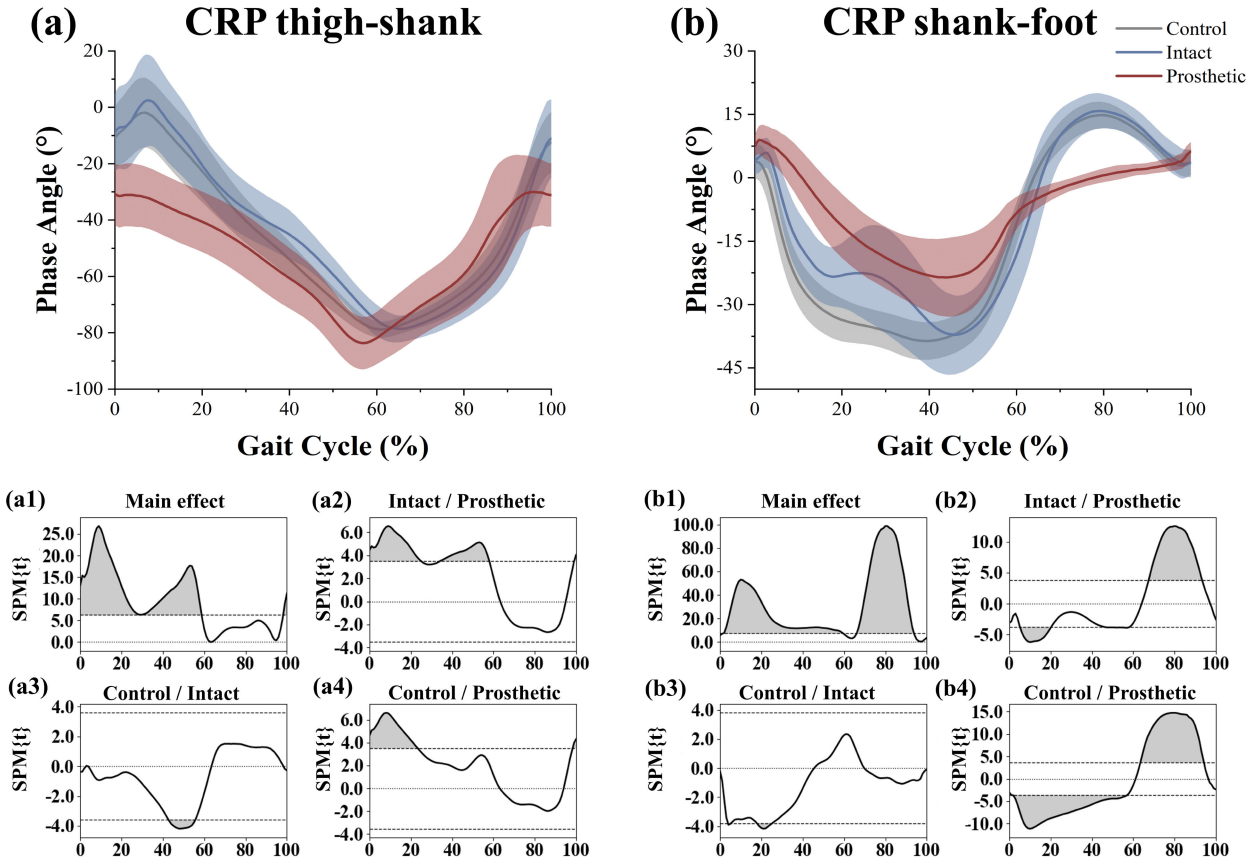

Fig. 2. Results of CRP curves and SPM analyses. The red and blue colors represent the prosthetic limbs and intact limbs, respectively. The black color represents the right limbs. The (a) and (b) are the CRP curves for thigh-shank and shank-foot couplings. In each CRP curve, the top plots are the CRP curves with standard deviations of the three limbs. The bottom four plots are the SPM results for main effect and post hoc test with Bonferroni correction. The shaded parts indicate significant differences. The bottom first plots (a1, b1) show the main effects among the three limbs (prosthetic limbs, intact limbs, and control limbs). The bottom second plots (a2, b2) show the statistical significance between intact limbs and prosthetic limbs. The bottom third plots (a3, b3) show the statistical significance between intact limbs and control limbs. The bottom fourth plots (a4, b4) show the statistical significance between control limbs and prosthetic limbs.

($p < 0.01$, intact: $34.76 \pm 7.50°$, prosthetic: $9.54 \pm 2.34°$, control: $25.68 \pm 7.65°$). The prosthetic limbs had a significantly smaller ankle range of motion than the other limbs ($p < 0.01$, intact: $42.24 \pm 4.70°$, prosthetic: $17.74 \pm 3.25°$, control: 33.28 ± 6.26). In regard to minimum segment angles, while no significant difference was observed in the thigh segments ($p = 0.14$), the prosthetic limbs had smaller minimum segment angles than the other limbs in the shank segment ($p < 0.01$, intact: $-54.16 \pm 4.38°$, prosthetic: $-60.22 \pm 4.21°$, control: $-55.58 \pm 2.65°$). Furthermore, in the foot segment, the intact limbs had significantly smaller minimum segment angles than the other limbs, and the prosthetic limbs had significantly higher minimum segment angles than the other limbs ($p < 0.01$, intact: $-18.68 \pm 6.37°$, prosthetic: $3.59 \pm 6.80°$, control: $-7.21 \pm 7.64°$). The prosthetic thigh segments exhibited a larger range of motion than the control ($p = 0.01$, intact: $52.07 \pm 3.76°$, prosthetic: $54.67 \pm 4.45°$, control: $49.67 \pm 3.76°$), while the prosthetic limbs had a significantly larger shank range of motion than the other two limbs ($p < 0.01$, intact: $77.00 \pm 4.67°$, prosthetic: $84.19 \pm 4.66°$, control: $76.94 \pm 3.53°$). In regard to the foot segment range of motion, both the prosthetic limbs and intact limbs exhibited significant differences from the control limbs ($p < 0.01$, intact: $112.85 \pm 6.71°$, prosthetic: $87.27 \pm 5.14°$, control: $98.35 \pm 7.61°$).

In regard to hip joint angle curves (Fig. 3 (a)), the main significant differences were observed in the first 20% of the gait cycle (Fig. 3 (a1)), and the post hoc test showed that during this period the intact limbs had a significantly larger flexion than that of the prosthetic limbs (Fig. 3 (a2)). The control limbs exhibited no significant difference between the intact and prosthetic limbs (Fig. 3 (a3-4)). For the knee joint angle curves (Fig. 3 (b)), a significant difference was found throughout the gait cycle (Fig. 3 (b1)). A lack of knee flexion during early stance for the prosthetic limbs was observed, and this was also significant in the post-hoc test from SPM (Fig. 3 (b2, b4)). Additionally, the prosthetic limbs hit the extension limit earlier than the intact and control limbs at around 90% of the gait cycle (Fig. 3 (b2)). Significance in the ankle joint curves (Fig. 3 (c)) was primarily observed during the pre-swing phase and initial-swing phase (Fig. 3 (c1)). In the thigh angle curves (supplementary Fig. S1 (a)), significant differences were evident in the early stance and swing phase (supplementary Fig. S2 (a1)). Notable significances were observed in the shank angle curve (supplementary Fig. S2 (a)) during the early stance phase and throughout the swing phase (supplementary Fig. S22 (b1)). Significant differences were found in the foot angle curve (supplementary Fig. S2 (a)) during the mid-stance phase and throughout the swing phase (supplementary Fig. S2 (c1)).

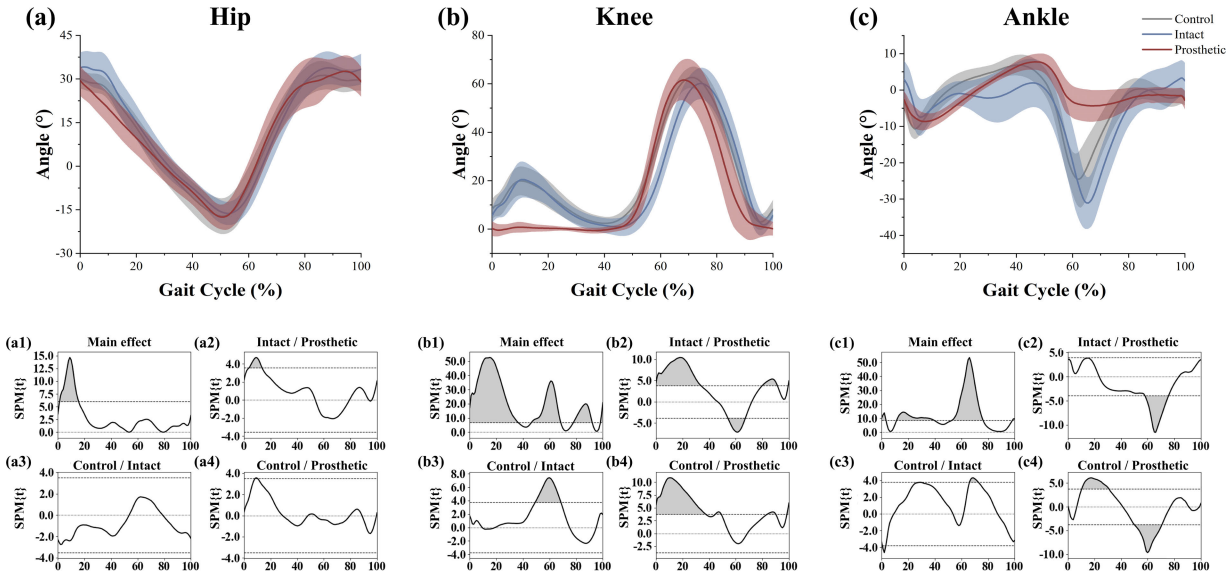

Fig. 3. Results of joint angles and SPM analyses. The red and blue colors represent prosthetic limbs and intact limbs, respectively. The black color represents the right limbs. The (a), (b), and (c) are results for hip, knee, and ankle joints. In each joint angle, the top plots are the joint angle curves with standard deviations of the three limbs. The bottom four plots are the SPM results for main effect and post hoc test with Bonferroni correction The shaded parts indicate significant differences. The bottom first plots (a1, b1, c1) show the main effects among the three limbs (prosthetic limbs, intact limbs, and control limbs). The bottom second plots (a2, b2, c2) show the statistical significance between intact limbs and prosthetic limbs. The bottom third plots (a3, b3, c3) show the statistical significance between intact limbs and control limbs. The bottom fourth plots (a4, b4, c4) show the statistical significance between control limbs and prosthetic limbs.

IV. Discussion

This study investigated the lower-limb coordination of individuals with uTFA and non-disabled individuals during walking. Two hypotheses were proposed regarding the thigh-shank and shank-foot couplings. In the thigh-shank coupling, prosthetic limbs were hypothesized to demonstrate larger MARP with smaller DP than the other two limbs. In shank-foot coupling, prosthetic limbs were hypothesized to demonstrate smaller MARP and DP than the other two limbs. In non-disabled individuals, MARP and DP between the lower limbs were hypothesized to be similar. The first hypothesis was not supported as the three limbs exhibited no significant differences in the MARP, while the prosthetic exhibited smaller DP than intact and control limbs. The second hypothesis was partially supported since the prosthetic limbs exhibited more in-phase (smaller MARP) coordination patterns and smaller DP than the other two limbs. Thus, the results of this study suggest that the individuals with uTFA could coordinate their thigh-shank coupling on two lower limbs as well as non-disabled individuals during walking. Different coordination patterns were induced by shank-foot couplings between prosthetic and intact limbs.

The regulation of unique gait patterns is revealed by CRP tools in individuals with uTFA. Surprisingly, in the thigh-shank coupling, the MARP of thigh-shank values revealed similar coordination patterns of thigh-shank coupling over the gait cycle for the three limbs. In the detailed view from the thigh-shank CRP curves, there lacks transition from the shank-leading pattern to the thigh-leading pattern of prosthetic limbs during the stance phase. However, this transition was identified during the swing phase when compared with the intact and control limbs. Same transition is also found during the sprinting gait of individuals with uTFA [25]. This could be the compensatory strategy of thigh-shank coupling to apply the different coordination features in the stance and swing phases to achieve a similar coordination pattern during gait. This could be explained as the prosthetic limb shank is a passive structure and thus relies on the thigh-leading pattern during the early stance phase for weight acceptance [28]. As for the swing phase differences, the intact and control limbs maintained the shank-leading pattern to prepare for heel strike. But at around 90% of the gait cycle, the prosthetic knee did not have adequate extension room (Fig. 2 (b)), and thus had to adopt the thigh-leading pattern to seek assistance from the thigh. The individuals with uTFA applied significantly different control strategies to achieve similar coordination patterns in the thigh-shank coupling of the lower limbs during the gait cycle.

In shank-foot coupling, the prosthetic limbs exhibited completely different coordination strategies than the other two limbs. The MARP shank-foot on the prosthetic limbs indicated that the prosthetic limbs applied a more in-phase coordination pattern during the gait cycle than the other limbs. This may suggest that prosthetic shank-foot coupling is more synchronized in prosthetic limbs [8]. However, it should be noted that this does not mean better coordination. In our study, the prosthetic shank and foot segments were passive structures and only rotate due to external forces. For example, an intact limb generates propulsive force at the end of the stance phase on the foot segment to the ground, while the lack of force generation of a prosthetic limb is partly compensated for by the intact limb [29]. In the shank-foot CRP curves, the prosthetic curve is closer to zero than for the other two limbs. This agrees with the significantly smaller MARP shank-foot value of the prosthetic limbs than that of the other limbs. A couple of distinct features were observed from the curves. First, the prosthetic limbs utilized foot-leading patterns throughout the swing phase while the other limbs switched to the shank-leading pattern at

around 80% of the gait cycle. This was because the prosthetic limbs were mainly influenced by the inertia force due to rotation and gravity. Both factors are consistent in producing a synchronized foot-shank coordination pattern of the prosthetic limbs, while the intact and control limbs during the terminal swing phase promote shank advancement to start the next gait cycle [30]. Thus, there is no coordination pattern switch of the shank-foot coupling of the prosthetic limbs during the swing phase. Another noticeable difference was observed during the mid-stance, where the coordination pattern of the intact limbs remained in the shank-leading pattern but fluctuated during 20% to 40% of the gait cycle when compared with the smooth shank-leading pattern of the prosthetic and control limbs. The fluctuation might be due to the increase in the foot-leading pattern during this period. This could be associated with the heel raising on the intact limbs from mid-stance to terminal stance. When the heel rises, an intact limb generates larger forces than the limb of non-disabled individuals forming a foot-leading pattern over a short period of time [30].

In this study, the variability of the coordination patterns provides additional insight for both the individuals with uTFA and non-disabled individuals. Larger DP might be associated with more involvement (e.g., force generation) of the limbs during gait. According to the definition of the CRP method, an excessively low DP value indicates a restricted coordination pattern [9]. A previous study on sprinting suggested that prosthetic limbs are more restricted than intact limbs [25]. The findings of this study are in line with the findings during running. This might suggest that during both walking and running, the prosthetic limbs are more restricted compared with the intact limbs.

Individuals with uTFA develop significantly different gait patterns between the lower limbs in gait kinematics and novel findings were illustrated with SPM analyses. The joint and segment angles' profiles in this study agreed well with the normative profile of the prosthetic walking gait reported in previous studies [29], [31]. In the ankle joint, the prosthetic limb exhibited a limited range of motion and peak plantar flexion angle. This is because a prosthetic ankle joint is a passive structure without ankle plantar flexors to generate active force for propulsion [32]. The hip and knee joints showed a similar range of motion and peak angle values among the three limbs. However, a lack of knee flexion of prosthetic limbs during the early stance was found. This is a common strategy when using prosthetic limbs in order to avoid experiencing large forces that may accidentally induce buckling during weight acceptance [33]. Additionally, differences in the range of motion were found between lower limbs using segment angles than using joint angles. Joint angles measure the relative orientation between two neighboring segments while the segment angles measure the absolute orientation of the corresponding segment. Our results indicate that segment angles are more sensitive in detecting changes when compared to joint angles. This is consistent with previous studies using segment angles for calculating CRP [15], [16], [17].

The findings of this study are expected to offer a new perspective on the coordination patterns for gait rehabilitation and prosthetic design. The gait rehabilitation program contains several steps with the aim of repeatedly practicing gait to rebuild the movement patterns. The findings and method of this study could be useful in gait evaluation and formulating training goals. Specifically, in the gait evaluation process, the CRP provides a new perspective regarding the coordination of movement. Changes in coordination patterns suggest alternations in the neuromusculoskeletal system. Hence CRP could be applied to evaluate the mastering of the prosthetic gait. In the gait training process, understanding the standard coordination profiles of the lower limb could provide a training target for prosthesis users. The prosthetic gait profile of experienced individuals with uTFA wearing prostheses could be used as a baseline to train individuals without experiences using uTFA to learn how to walk with prostheses with realistic goals. For example, after training, if the new prosthesis users show similar coordination patterns as the experienced prosthesis users, this might suggest maturity in the prosthetic gait. As for the application in prosthetic design, it is not reasonable to force a prosthetic limb to generate the same movement pattern as an intact limb, since a conventional prosthetic limb is a passive structure without actuators to control the segments [25]. But in newly developed powered prostheses and exoskeletons, forces/torques could be generated by motors with various control algorithms [34]. Optimizing the control algorithm for force generation by making segment angles and coordination patterns closer to the intact limbs or the limbs of non-disabled individuals may be a solution for better prosthesis design.

This study has several limitations. Firstly, the cause of amputation varied among the participants. This factor was suggested to influence certain gait parameters. For instance, the vascular type of amputation is believed to result in slower walking speed and shorter stride length compared to traumatic amputation [35]. Secondly, the residual limb length was not consistent in the individuals with uTFA. The femoral length may affect the gait parameters, with shorter residual limb lengths being associated with a larger hip abduction angle [36]. Thirdly, this study only examined kinematic data via CRP analysis in the sagittal plane. Subsequent studies should incorporate other planes (transverse and/or coronal planes) to enrich the knowledge of coordination in walking among individuals with uTFA. Finally, the profiles of the prosthetic knees and feet influence the kinematics. The hydraulic/ pneumatic knees with or without microprocessor control, and prosthetic feet in various shapes and materials, can affect segmental kinematics during walking [37], [38].

V. Conclusion

In summary, individuals with uTFA use compensatory strategies during the stance and swing phases to achieve similar coordination patterns of the lower limbs in thigh-shank coupling while walking. Specifically, to counterbalance the insufficient force generation in the prosthetic shank, the prosthetic thigh-shank employs a consistent thigh-leading pattern during the entire stance phase, while the intact limb transitions from shank-leading to thigh-leading within the same phase. During the swing phase, a prosthetic limb transitions from shank-leading to thigh-leading, while the intact limb consistently exhibits a shank-leading pattern through the entire swing phase. These distinct coordination characteristics help achieve similar coordination patterns during gait. In shank-foot

coupling, a prosthetic limb exhibits a more in-phase coordination pattern and improved synchronization due to its passive structure, compared to an intact limb with active muscles. The findings of this study can provide novel insights into prosthetic gait rehabilitation and the development of prosthetic devices with a better understanding of lower-limb movement coordination.

Supplementary Materials

Supplementary Fig. S1. Illustration of the calculation of CRP thigh-shank coupling using Hilbert transform.

Supplementary Fig. S2. Results of segment angles and SPM analyses.

Figure caption for supplementary files.

References

[1] I.-C. Lee, M. M. Pacheco, M. D. Lewek, and H. Huang, "Perceiving amputee gait from biological motion: Kinematics cues and effect of experience level," *Sci. Rep.*, vol. 10, no. 1, p. 17093, Oct. 2020.

[2] T. Kobayashi et al., "Effects of walking speed on magnitude and symmetry of ground reaction forces in individuals with transfemoral prosthesis," *J. Biomech.*, vol. 130, Jan. 2022, Art. no. 110845.

[3] V. J. Harandi et al., "Gait compensatory mechanisms in unilateral transfemoral amputees," *Med. Eng. Phys.*, vol. 77, pp. 95–106, Mar. 2020.

[4] C. De Marchis et al., "Characterizing the gait of people with different types of amputation and prosthetic components through multimodal measurements: A methodological perspective," *Frontiers Rehabil. Sci.*, vol. 3, Mar. 2022, Art. no. 804746.

[5] S. A. Gard, "Use of quantitative gait analysis for the evaluation of prosthetic walking performance," *J. Prosthetics Orthotics*, vol. 18, no. 6, pp. P93–P104, Jan. 2006.

[6] E. R. Esposito and R. H. Miller, "Maintenance of muscle strength retains a normal metabolic cost in simulated walking after transtibial limb loss," *PLoS ONE*, vol. 13, no. 1, Jan. 2018, Art. no. e0191310.

[7] H. Gholizadeh, N. A. A. Osman, A. Eshraghi, S. Ali, and N. A. Razak, "Transtibial prosthesis suspension systems: Systematic review of literature," *Clin. Biomech.*, vol. 29, no. 1, pp. 87–97, Jan. 2014.

[8] N. Stergiou, *Innovative Analyses of Human Movement*. Champaign, IL, USA: Human Kinetics Publishers, 2004.

[9] M. Hu, T. Kobayashi, J. Zhou, and W.-K. Lam, "Current application of continuous relative phase in running and jumping studies: A systematic review," *Gait Posture*, vol. 90, pp. 215–233, Oct. 2021.

[10] M. Schaarschmidt, S. W. Lipfert, C. Meier-Gratz, H.-C. Scholle, and A. Seyfarth, "Functional gait asymmetry of unilateral transfemoral amputees," *Hum. Movement Sci.*, vol. 31, no. 4, pp. 907–917, Aug. 2012.

[11] Y. Chang et al., "Changes in spatiotemporal parameters and lower limb coordination during prosthetic gait training in unilateral transfemoral amputees," *Int. J. Precis. Eng. Manuf.*, vol. 23, no. 3, pp. 361–373, Mar. 2022.

[12] E. Lathouwers et al., "Continuous relative phases of walking with an articulated passive ankle–foot prosthesis in individuals with a unilateral transfemoral and transtibial amputation: An explorative case–control study," *Biomed. Eng. OnLine*, vol. 22, no. 1, p. 14, Feb. 2023.

[13] Z. Xu et al., "Lower limb inter-joint coordination of unilateral transfemoral amputees: Implications for adaptation control," *Appl. Sci.*, vol. 10, no. 12, p. 4072, Jun. 2020.

[14] J. A. S. Kelso and B. Tuller, "A dynamical basis for action systems," in *Handbook of Cognitive Neuroscience*, M. S. Gazzaniga, Ed. Boston, MA, USA: Springer, 1984, doi: 10.1007/978-1-4899-2177-2_16.

[15] J. E. Clark and S. J. Phillips, "A longitudinal study of intralimb coordination in the first year of independent walking: A dynamical systems analysis," *Child Develop.*, vol. 64, no. 4, pp. 1143–1157, Aug. 1993.

[16] P. N. Kugler, J. A. S. Kelso, and M. T. Turvey, "1 on the concept of coordinative structures as dissipative structures: I. Theoretical lines of convergence," in *Advances in Psychology*. Amsterdam, The Netherlands: Elsevier, 1980, pp. 3–47.

[17] J. M. Haddad, R. E. A. van Emmerik, J. S. Wheat, J. Hamill, and W. Snapp-Childs, "Relative phase coordination analysis in the assessment of dynamic gait symmetry," *J. Appl. Biomech.*, vol. 26, no. 1, pp. 109–113, Feb. 2010.

[18] T. C. Pataky, "One-dimensional statistical parametric mapping in Python," *Comput. Methods Biomech. Biomed. Eng.*, vol. 15, no. 3, pp. 295–301, Mar. 2012.

[19] T. C. Pataky, "Generalized n-dimensional biomechanical field analysis using statistical parametric mapping," *J. Biomech.*, vol. 43, no. 10, pp. 1976–1982, Jul. 2010.

[20] A. Herbaut, P. Chavet, M. Roux, N. Guéguen, F. Barbier, and E. Simoneau-Buessinger, "The influence of shoe aging on children running biomechanics," *Gait Posture*, vol. 56, pp. 123–128, Jul. 2017.

[21] S. R. Pinhey, H. Murata, G. Hisano, D. Ichimura, H. Hobara, and M. J. Major, "Effects of walking speed and prosthetic knee control type on external mechanical work in transfemoral prosthesis users," *J. Biomech.*, vol. 134, Mar. 2022, Art. no. 110984.

[22] Y. Kobayashi, N. Hida, K. Nakajima, M. Fujimoto, and M. Mochimaru, "AIST gait database 2019," Nat. Inst. Adv. Ind. Sci. Technol. (AIST), Kashiwa, Japan, 2019. [Online]. Available: https://unit.aist.go.jp/harc/ExPART/GDB2019.html

[23] M. P. Kadaba, H. K. Ramakrishnan, and M. E. Wootten, "Measurement of lower extremity kinematics during level walking," *J. Orthopaedic Res.*, vol. 8, no. 3, pp. 383–392, May 1990.

[24] P. F. Lamb and M. Stöckl, "On the use of continuous relative phase: Review of current approaches and outline for a new standard," *Clin. Biomech.*, vol. 29, no. 5, pp. 484–493, May 2014.

[25] M. Hu, T. Kobayashi, G. Hisano, H. Murata, D. Ichimura, and H. Hobara, "Sprinting performance of individuals with unilateral transfemoral amputation: Compensation strategies for lower limb coordination," *Roy. Soc. Open Sci.*, vol. 10, no. 3, Mar. 2023, Art. no. 221198.

[26] T. C. Pataky, M. A. Robinson, and J. Vanrenterghem, "Region-of-interest analyses of one-dimensional biomechanical trajectories: Bridging 0D and 1D theory, augmenting statistical power," *PeerJ*, vol. 4, Nov. 2016, Art. no. e2652.

[27] T. C. Pataky, J. Vanrenterghem, and M. A. Robinson, "Zero- vs. one-dimensional, parametric vs. non-parametric, and confidence interval vs. hypothesis testing procedures in one-dimensional biomechanical trajectory analysis," *J. Biomech.*, vol. 48, no. 7, pp. 1277–1285, May 2015.

[28] Y. Motomura et al., "Effect of different knee flexion angles with a constant hip and knee torque on the muscle forces and neuromuscular activities of hamstrings and gluteus maximus muscles," *Eur. J. Appl. Physiol.*, vol. 119, no. 2, pp. 399–407, Feb. 2019.

[29] T. Kobayashi, G. Hisano, Y. Namiki, S. Hashizume, and H. Hobara, "Walking characteristics of runners with a transfemoral or knee-disarticulation prosthesis," *Clin. Biomech.*, vol. 80, Dec. 2020, Art. no. 105132.

[30] J. Perry and J. M. Burnfield, *Gait Analysis: Normal and Pathological Function*, 2nd ed. San Francisco, CA, USA: Slack, 2010.

[31] S. Ranaldi et al., "Characterization of prosthetic knees through a low-dimensional description of gait kinematics," *J. NeuroEng. Rehabil.*, vol. 20, no. 1, p. 46, Apr. 2023.

[32] J. R. Yang, H. S. Yang, D. H. Ahn, D. Y. Ahn, W. S. Sim, and H.-E. Yang, "Differences in gait patterns of unilateral transtibial amputees with two types of energy storing prosthetic feet," *Ann. Rehabil. Med.*, vol. 42, no. 4, pp. 609–616, Aug. 2018.

[33] R. Amma, G. Hisano, H. Murata, M. J. Major, H. Takemura, and H. Hobara, "Inter-limb weight transfer strategy during walking after unilateral transfemoral amputation," *Sci. Rep.*, vol. 11, no. 1, p. 4793, Feb. 2021.

[34] M. K. Ishmael et al., "Powered hip exoskeleton reduces residual hip effort without affecting kinematics and balance in individuals with above-knee amputations during walking," *IEEE Trans. Biomed. Eng.*, vol. 70, no. 4, pp. 1162–1171, Apr. 2023.

[35] B. J. Hafner, J. E. Sanders, J. Czerniecki, and J. Fergason, "Energy storage and return prostheses: Does patient perception correlate with biomechanical analysis?" *Clin. Biomech.*, vol. 17, no. 5, pp. 325–344, Jun. 2002.

[36] J. C. Bell, E. J. Wolf, B. L. Schnall, J. E. Tis, L. L. Tis, and M. B. K. Potter, "Transfemoral amputations: The effect of residual limb length and orientation on gait analysis outcome measures," *J. Bone Joint Surg.*, vol. 95, no. 5, pp. 408–414, 2013.

[37] V. Creylman, I. Knippels, P. Janssen, E. Biesbrouck, K. Lechler, and L. Peeraer, "Assessment of transfemoral amputees using a passive microprocessor-controlled knee versus an active powered microprocessor-controlled knee for level walking," *Biomed. Eng. OnLine*, vol. 15, no. S3, pp. 53–63, Dec. 2016.

[38] H. Goujon et al., "A functional evaluation of prosthetic foot kinematics during lower-limb amputee gait," *Prosthetics Orthotics Int.*, vol. 30, no. 2, pp. 213–223, 2006.